Supplementary Information for:

Quantitative determination of carbonaceous particle mixing state in Paris using single particle mass spectrometer and aerosol mass spectrometer measurements

Robert M. Healy[1,2], Jean Sciare[3], Laurent Poulain[4], Monica Crippa[5], Alfred Wiedensohler[4], Andre S. H. Prévôt[5], Roland Sarda-Estève[3], Maygan L. McGuire[2], Cheol-Heon Jeong[2], Eoin McGillicuddy[1], Ian P. O'Connor[1], John R. Sodeau[1], Greg J. Evans[2], John C. Wenger[1]

[1]*Department of Chemistry and Environmental Research Institute, University College Cork, Ireland*

[2]*Southern Ontario Centre for Atmospheric Aerosol Research, University of Toronto, 200 College Street, Toronto, Ontario, Canada*

[3]*LSCE, Laboratoire des Sciences du Climat et de l'Environnement, CEA-CNRS-UVSQ, Gif-sur-Yvette, France*

[4]*Leibniz Institute for Tropospheric Research, Leipzig, Germany*

[5]*Laboratory of Atmospheric Chemistry, Paul Scherrer Institute, PSI Villigen, 5232, Switzerland*

Corresponding author email address:

robert.healy@utoronto.ca

ATOFMS scaling procedures

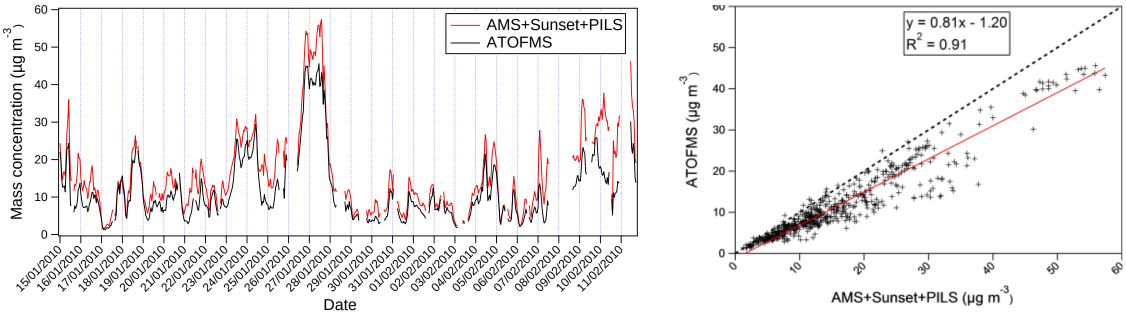

Fig. S1: Temporal trends and correlation for the summed mass concentration of all ten ATOFMS carbonaceous classes and the summed mass concentration of EC, OA, ammonium, sulphate, nitrate, chloride, potassium and sodium measured by the Sunset OCEC analyser, the HR-ToF-AMS and the PILS. The red line represents the orthogonal distance regression fit and the dashed black line represents a 1:1 fit.

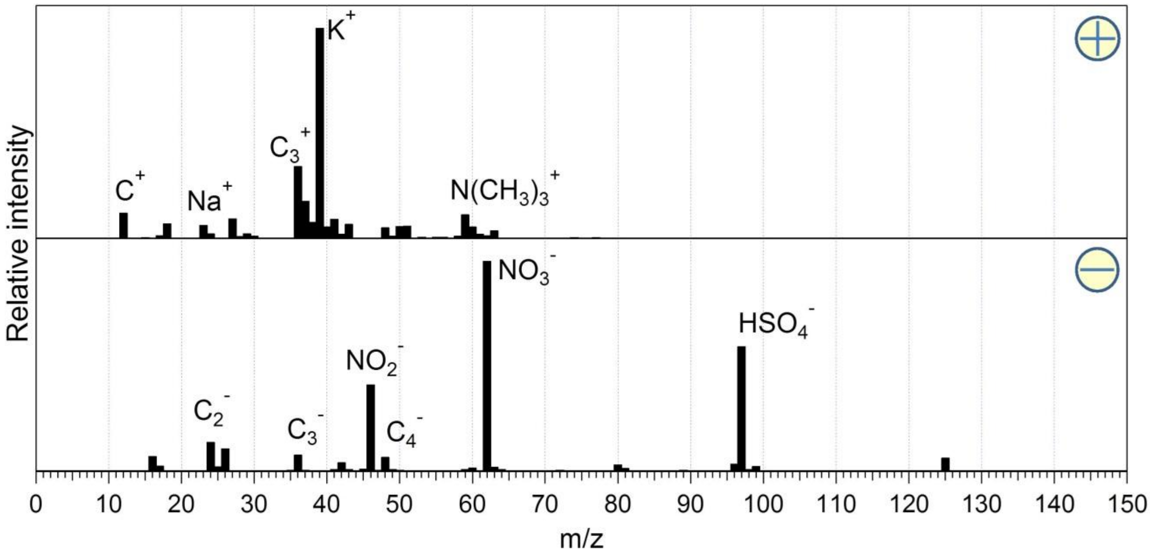

Fig. S2: Number-weighted average mass spectrum of the 1.50 million carbonaceous single particles used to obtain relative sensitivity factors for the six species quantified.

Sensitivity analysis using seven day subsets of the ATOFMS dataset

The suitability of the ATOFMS quantification approach to predict the variability and mass concentrations of the six chemical species was tested by selecting seven day subsets of the four week dataset, and comparing these to the average mass concentrations measured by the HR-ToF-AMS, Sunset and PILS instruments for the same period. The relative sensitivity factors (RSFs) obtained were then used to predict mass concentrations of each species for all four weeks. The variability of each species was reproduced very well despite the subset chosen, as shown in Table S1. However, the slopes were observed to vary significantly depending on the subset. This can be explained by examining the classes that are prevalent during each seven day period. The subset from week 2, for example, produces reconstructed mass concentrations for each species that are most similar to those produced by the full dataset, with the exception of potassium. This week (22/01/2010-29/01/2010) was influenced by both marine and continental air masses (Fig. 4), and thus all ten mixing states are well represented in the average mass spectrum generated. Conversely, a much greater divergence is observed when using the subset from week 3 (29/01/2010-05/02/2010), because this period was influenced almost exclusively by marine air masses and the single particle classes associated with continental transport have minimal contribution to the average mass spectrum generated. Thus, the quantification approach described here is expected to be most accurate when the dataset used for prediction is as large as possible, encompassing differences in mixing state that occur due to changes in meteorology and air mass origin. Thick secondary coatings have been demonstrated to affect RSF values for internally mixed species detected by ATOFMS (Pratt and Prather, 2009). Therefore RSFs are expected to vary significantly depending upon season and receptor site location.

Table S1: Comparison of ATOFMS-derived, HR-ToF-AMS, PILS and Sunset mass concentrations for OA, EC and inorganic ions derived using seven day subsets. Results for the full ATOFMS dataset are also included for comparison.

Species	SO_4		NO_3		NH_4		OA		EC		K	
	R^2	slope	R^2	slope	R^2	slope	R^2	slope	R^2	slope	R^2	slope
Week 1	0.78	0.58	0.67	0.70	0.78	0.76	0.75	1.25	0.71	1.49	0.78	0.64
Week 2	0.79	0.75	0.68	0.81	0.80	0.71	0.75	1.10	0.75	1.17	0.78	1.27
Week 3	0.79	0.50	0.67	0.50	0.81	0.70	0.75	1.54	0.73	1.54	0.79	0.65
Week 4	0.78	0.88	0.68	0.93	0.81	0.96	0.77	0.89	0.75	0.72	0.77	0.66
All data	0.78	0.66	0.67	0.78	0.78	0.82	0.75	1.16	0.72	1.14	0.78	0.76

Effect of scaling upon relative contributions of each particle class

A single mass-weighted average mass spectrum generated from the 10 classes was expected to give a more representative contribution of each class to $PM_{0.15-1}$ for the measurement period. However, the average mass spectrum obtained was almost identical to that obtained using a number-weighted average (Fig. S2). This can be explained by the similarity of the relative contributions shown in Fig. S3.

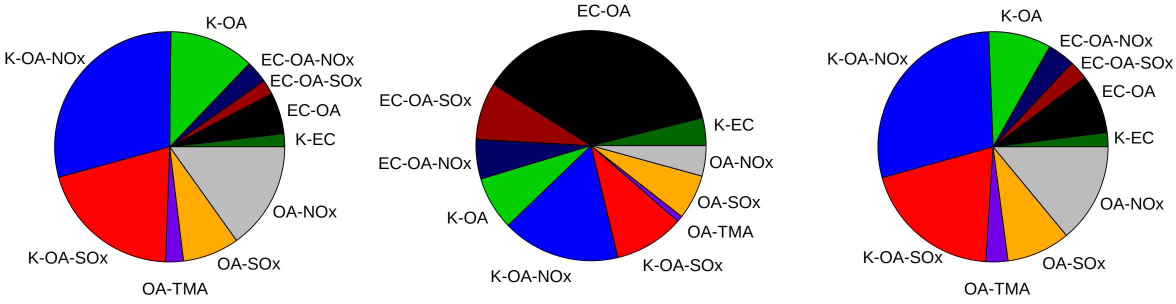

Fig. S3: Relative unscaled particle number (left), scaled particle number (middle) and scaled particle mass concentration (right) for the 10 carbonaceous ATOFMS particle classes.

When the ATOFMS particle counts are scaled to account for size-dependent detection efficiency, the relative number concentrations of the smaller EC-rich particles increases significantly. However, once these scaled number concentrations are converted to volume and mass concentrations, the relative contribution of the smaller particles decreases, approaching the original ratios. It is important to note that this may not be the case for ATOFMS studies performed in locations impacted significantly by larger crustal or sea salt particles, but these findings are encouraging for urban ATOFMS source apportionment studies where scaling ATOFMS particle number concentration data is not an option. Using the mass-weighted average mass spectrum for the quantification procedure gave results that were highly similar to those obtained using the number-weighted average mass spectrum, as shown in Table S2.

Table S2: Comparison of ATOFMS-derived, HR-ToF-AMS, PILS and Sunset mass concentrations for OA, EC and inorganic ions derived using a number-weighted and mass-weighted average mass spectrum.

Species	SO_4		NO_3		NH_4		OA		EC		K	
	R^2	slope	R^2	slope	R^2	slope	R^2	slope	R^2	slope	R^2	slope
Number	0.78	0.66	0.67	0.78	0.78	0.82	0.75	1.16	0.72	1.14	0.78	0.76
Mass	0.78	0.65	0.67	0.81	0.78	0.83	0.75	1.16	0.72	1.03	0.77	0.83

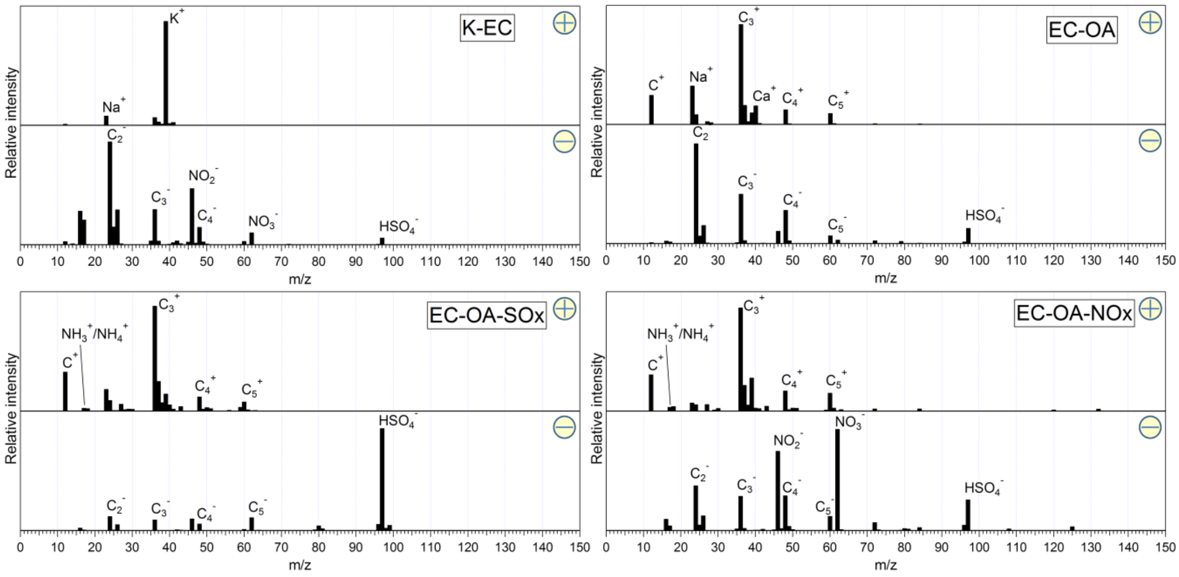

Fig. S4: Average mass spectra for the 4 EC classes described in detail in Healy et al. (2012). Note that K-EC and EC-OA were termed ‘ECbiomass’ and ‘ECtraffic’ in the previous manuscript, respectively.

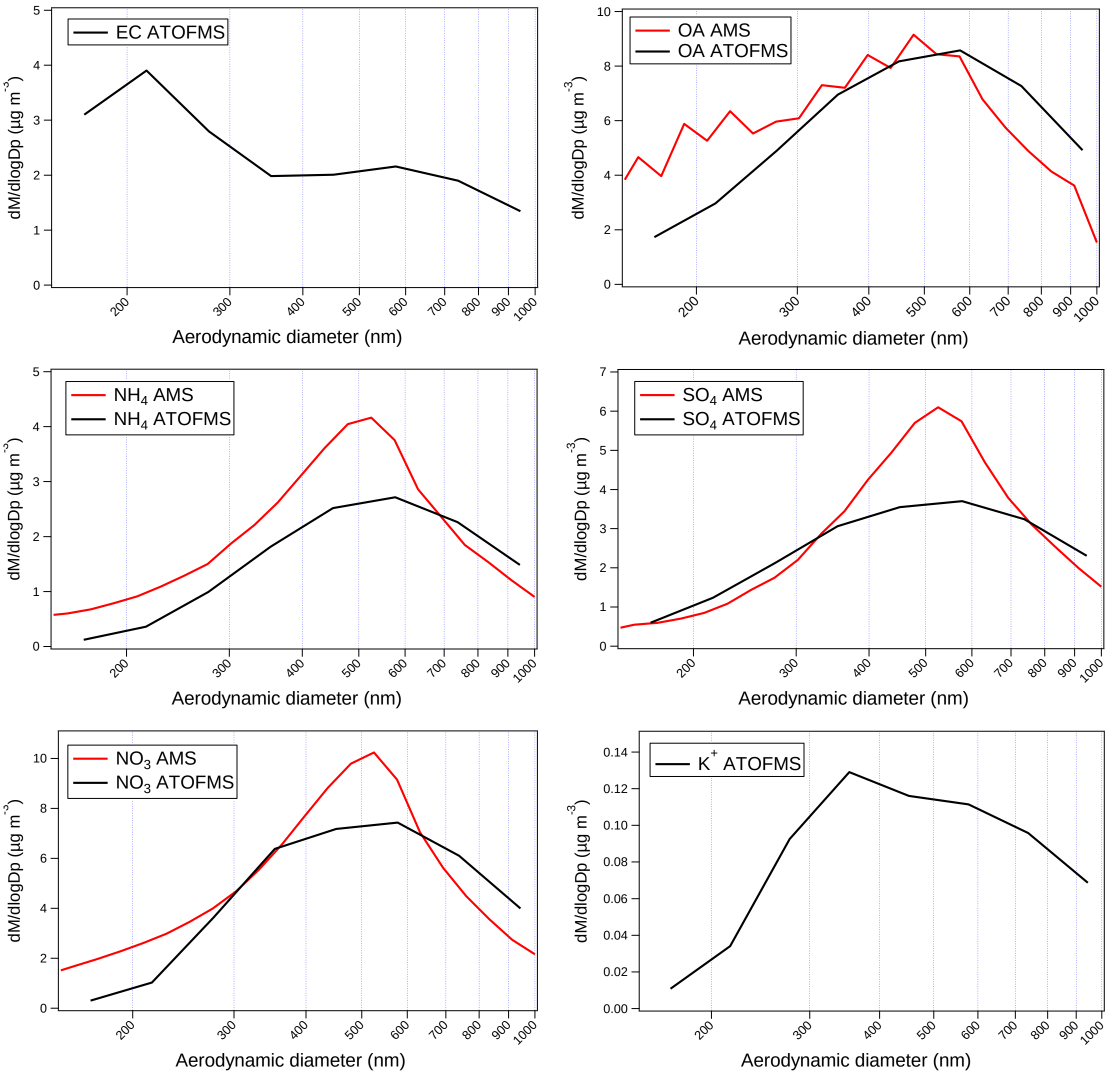

Fig. S5: Average ATOFMS-derived size-resolved mass concentrations for each species (black) and HR-ToF-AMS size-resolved mass concentrations for OA and inorganic ions (red).

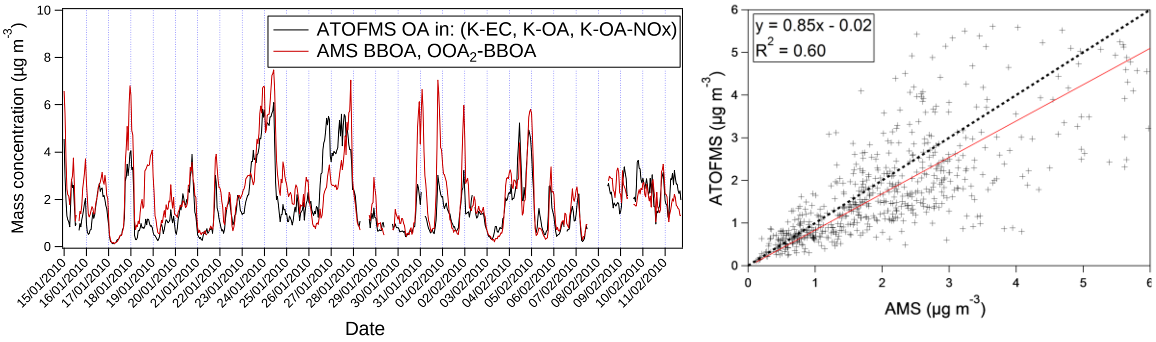

Fig. S6: Comparison of the summed mass concentration of the HR-ToF-AMS BBOA and OOA_2_BBOA PMF factors with summed OA content from the ATOFMS K-EC, K-OA and K-OA-NOx single particle classes. The red line represents the orthogonal distance regression fit and the black dashed line represents the 1:1 ratio.

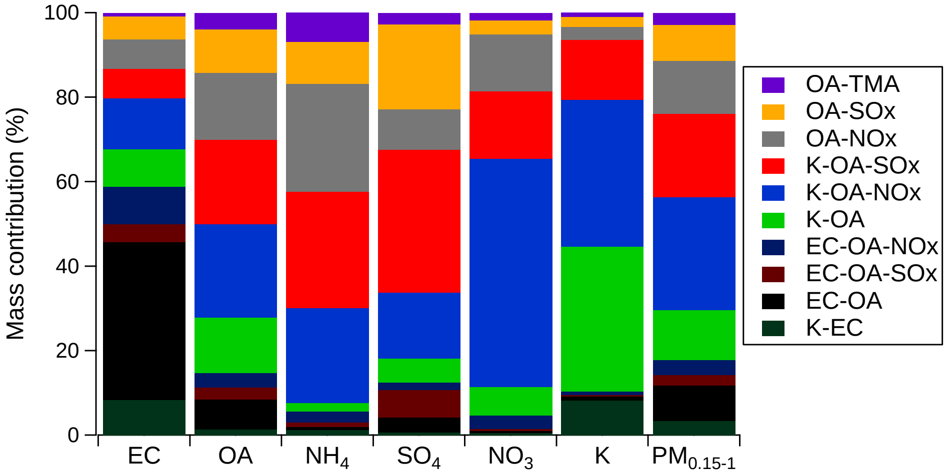

Fig. S7. Relative mass contributions (%) of each ATOFMS class to each chemical species and total reconstructed mass.

Table S3. Relative mass contributions (%) of each ATOFMS class to each chemical species and total reconstructed mass.

ATOFMS class	EC	OA	NH_4	SO_4	NO_3	K	$PM_{0.15-1}$
K-EC	8	1	1	1	1	8	3
EC-OA	37	7	1	4	0	1	8
EC-OA-SOx	4	3	1	6	0	0	3
EC-OA-NOx	9	4	3	2	3	1	3
K-OA	9	13	2	6	7	34	12
K-OA-NOx	12	22	22	16	54	35	27
K-OA-SOx	7	20	28	34	16	14	20
OA-NOx	7	16	26	10	14	3	12
OA-SOx	5	10	10	20	3	2	9
OA-TMA	1	4	7	3	2	1	3

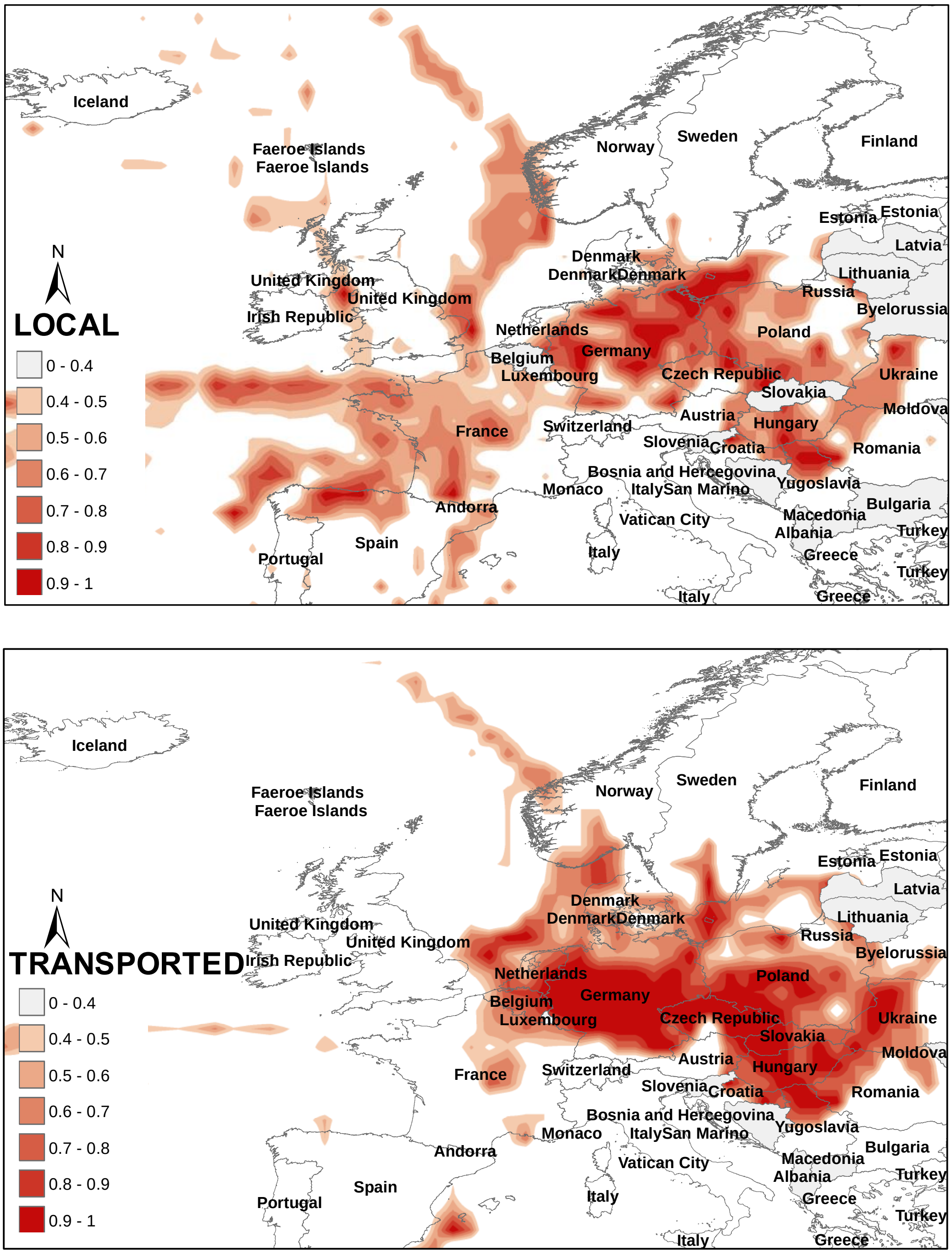

Fig. S8: Potential source contribution function plot for local and transported particles discussed in Section 3.4.

References

Pratt, K. A., and Prather, K. A.: Real-Time, Single-Particle Volatility, Size, and Chemical Composition Measurements of Aged Urban Aerosols, Environmental Science & Technology, 43, 8276-8282, 10.1021/es902002t, 2009.